ANZIAM J. 58(2017), 256–264
doi:10.1017/S1446181116000341

THE MELLIN CENTRAL PROJECTION TRANSFORM

JIANWEI YANG[✉1], LIANG ZHANG[1] and ZHENGDA LU[1]

(Received 12 June, 2016; accepted 15 October, 2016; first published online 7 March 2017)

Abstract

The central projection transform can be employed to extract invariant features by combining contour-based and region-based methods. However, the central projection transform only considers the accumulation of the pixels along the radial direction. Consequently, information along the radial direction is inevitably lost. In this paper, we propose the Mellin central projection transform to extract affine invariant features. The radial factor introduced by the Mellin transform, makes up for the loss of information along the radial direction by the central projection transform. The Mellin central projection transform can convert any object into a closed curve as a central projection transform, so the central projection transform is only a special case of the Mellin central projection transform. We prove that closed curves extracted from the original image and the affine transformed image by the Mellin central projection transform satisfy the same affine transform relationship. A method is provided for the extraction of affine invariants by employing the area of closed curves derived by the Mellin central projection transform. Experiments have been conducted on some printed Chinese characters and the results establish the invariance and robustness of the extracted features.

2010 *Mathematics subject classification*: 68T10.

Keywords and phrases: Mellin central projection transform, Mellin transform, affine invariants, feature extraction.

1. Introduction

Images of an object taken from different viewpoints often suffer from perspective distortions [1, 3]. The affine model is a reasonable approximation if the object is small compared with the camera-to-scene distance. An affine transform is defined as

$$\begin{pmatrix}\widetilde{x}\\ \widetilde{y}\end{pmatrix} = \begin{pmatrix}a & b\\ c & d\end{pmatrix}\begin{pmatrix}x\\ y\end{pmatrix} + \begin{pmatrix}e\\ f\end{pmatrix} = A\begin{pmatrix}x\\ y\end{pmatrix} + \begin{pmatrix}e\\ f\end{pmatrix}, \tag{1.1}$$

where A is a nonsingular matrix. A similarity transform, which includes rotation, scaling and translation, is only a special case of an affine transform [3].

[1]School of Mathematics and Statistics, Nanjing University of Information Science and Technology, Nanjing, China, 210044; e-mail: yjianw@nuist.edu.cn.

In pattern recognition and computer vision, the extraction of affine features plays a very important role. Many methods, which can be classified into region-based methods and contour-based methods, have been developed.

The contour-based methods provide better data reduction. There are many examples of these approaches, which include Fourier descriptors [1] and wavelet descriptors [7]. However, the performance of these contour-based methods is strongly dependent on the success of the boundary extraction process. Most of these contour-based methods can only be applied to objects with a single boundary instead of objects with several separable components. In contrast to contour-based methods, region-based techniques take all pixels of the image into account. The moment-invariant methods are the most widely used techniques. The commonly used affine moment invariants (AMIs) [3] are extensions of the classical moment invariants. Teh and Chin [13] have shown that high-order moments are more vulnerable to white noise than low-order moments. This makes their use undesirable in pattern recognition. Some novel region-based methods have also been proposed to extract affine invariant features. These methods give high accuracy, but usually at the expense of high complexity.

The contour-based and region-based methods both have their advantages and disadvantages. Thus, an intuitive way is to combine them together. The *central projection transform* (CPT), which was first proposed by Tang [12], can be used to convert any object into a closed curve. As a result, contour-based method can be applied to the closed curve obtained by the CPT for the extraction of affine invariants. Lan and Yang [8] have employed the CPT, the whitening transform and the Fourier transform to extract affine invariants. But objects of completely different appearances may have the same closed curves as the ones obtained by the CPT. In Figure 1, we show examples of different images with the same CPT, because the CPT is, in fact, equal to the accumulation of the pixels along different angles. Consequently, information along radial directions has been lost. To solve this problem, a radial factor is introduced by employing the Mellin transform in this paper.

There have been many attempts to apply the Mellin transform for the extraction of invariant features (see, for example, [2, 4, 6, 11]). However, up to now, this transform has only been used to extract invariants of a similarity transform. In this paper, we apply the Mellin transform to extract affine invariant features.

We propose the *Mellin central projection transform* (MCPT) to extract affine invariant features. By the MCPT, any object can be converted into a closed curve. The CPT is only a special case of the proposed MCPT. We prove that a closed curve extracted from the affine transformed image is the same affine transformed version of that extracted from the original image by the MCPT. The area of a closed curve obtained by the MCPT is used to construct affine invariants. The results of our experiment demonstrate that the obtained affine invariants have stronger robustness than traditional moments.

The paper is organized as follows. In Section 2, we introduce the MCPT and analyse some properties of MCPT. A method is also presented for the extraction of affine invariant features. In Section 3, the experimental results are described. The paper concludes with a brief summary in Section 4.

https://doi.org/10.1017/S1446181116000341 Published online by Cambridge University Press

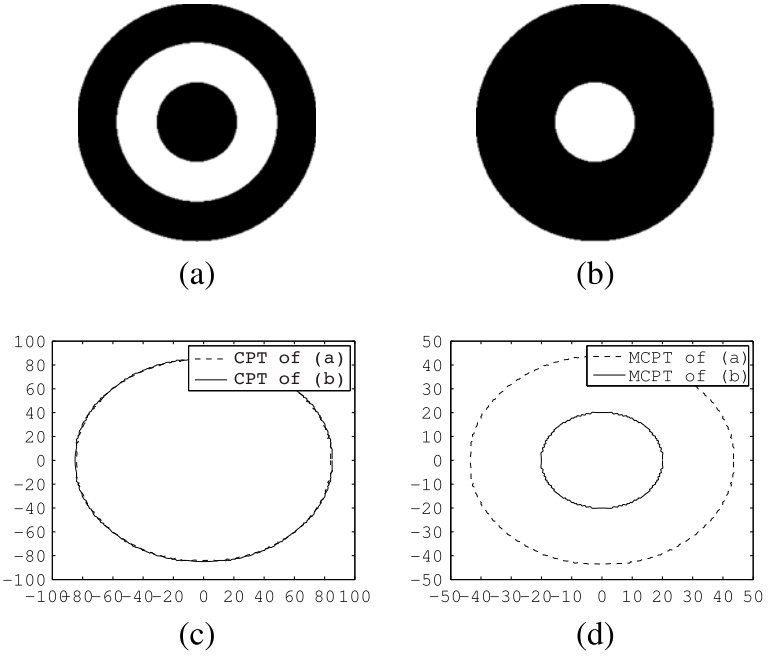

FIGURE 1. Two images ((a) and (b)), their central projection transforms (c) and their Mellin central projection transforms (d).

2. The MCPT method and its properties

2.1. The definition of the MCPT We set the origin at the centroid of the image and transform to polar coordinates (r, θ) with

$$x = r\cos\theta, \quad y = r\sin\theta.$$

Hence, the image can be represented by a function f of r and θ, namely, $f(r, \theta)$. The CPT of $f(r, \theta)$ is given by

$$g(\theta) = \int_0^\infty f(r, \theta)\, dr, \tag{2.1}$$

where $\theta \in [0, 2\pi)$. By equation (2.1), a single value corresponds to an angle $\theta \in [0, 2\pi)$. Consequently, a closed curve can be derived from any object by employing the CPT, which was used to extract invariant features by Lan and Yang [8] and Tang et al. [12].

As previously mentioned, objects with different appearances may have the same CPT. In Figure 1, two different images (Figures 1(a) and 1(b)) derive the same closed curve by the CPT (Figure 1(c)). This is because the function $g(\theta)$ in equation (2.1) is the integral along the radial direction without the radial factor r. Consequently, information along radial directions has been lost. In this paper, we introduce a radial factor by employing the Mellin transform.

https://doi.org/10.1017/S1446181116000341 Published online by Cambridge University Press

Let $h(x) \in \mathbb{R}$ be a real-valued function; the Mellin transform of h is defined as [5]

$$M_h(s) = \int_0^\infty h(x) x^{s-1}\, dx \tag{2.2}$$

with $s = \sigma + \tau i$, where σ is a constant that makes the integral in equation (2.2) convergent and τ is a variable.

Definition 2.1. The MCPT of image $f(r, \theta)$ is defined as

$$Mg_f^s(\theta) = \left| \int_0^\infty r^{s-1} f(r, \theta)\, dr \right|^{1/\sigma},$$

where $s = \sigma + \tau i$ with $\sigma > 0$.

For a fixed complex number s, the set $\{(\theta, Mg_f^s(\theta) \mid \theta \in [0, 2\pi)\}$ constitutes a closed curve, as θ changes from zero to 2π. Consequently, any object can be converted into a closed curve by the MCPT. If we set $s = 1$, then

$$Mg_f^s(\theta) = \left| \int_0^\infty r^{1-1} f(r, \theta)\, dr \right| = \int_0^\infty f(r, \theta)\, dr = g(\theta).$$

In other words, the CPT is only a special case of the MCPT.

A radial factor r^{s-1} has been introduced in the definition of the MCPT. Some information along the radial direction can be kept in part. As shown in Figure 1(d) (s is set to $1 + 5i$), the MCPT converts the two different images in Figures 1(a) and 1(b) into two different closed curves.

2.2. Affine invariance of the MCPT The translation invariance is obtained by setting the origin at the centroid. As a result, equation (1.1) can be translated into

$$\begin{pmatrix} \widetilde{x} \\ \widetilde{y} \end{pmatrix} = A \begin{pmatrix} x \\ y \end{pmatrix}. \tag{2.3}$$

Let $(\tilde{r}, \tilde{\theta})$ be the corresponding polar coordinates with

$$\widetilde{x} = \widetilde{r} \cos \widetilde{\theta}, \quad \widetilde{y} = \widetilde{r} \sin \widetilde{\theta}, \tag{2.4}$$

where $\widetilde{\theta} \in [0, 2\pi)$.

Theorem 2.1. *For a complex number s, let $\tilde{f}(\widetilde{r}, \widetilde{\theta})$ be the affine transformed image of $f(r, \theta)$. Let $Mg_f^s(\theta)$ be the MCPT of $f(r, \theta)$ and let $\widetilde{Mg_f^s}(\widetilde{\theta})$ be the MCPT of $\tilde{f}(\widetilde{r}, \widetilde{\theta})$. Then*

$$\widetilde{Mg_f^s}(\widetilde{\theta}) \cos \widetilde{\theta} = a Mg_f^s(\theta) \cos \theta + b Mg_f^s(\theta) \sin \theta,$$
$$\widetilde{Mg_f^s}(\widetilde{\theta}) \sin \widetilde{\theta} = c Mg_f^s(\theta) \cos \theta + d Mg_f^s(\theta) \sin \theta.$$

https://doi.org/10.1017/S1446181116000341 Published online by Cambridge University Press

PROOF. From equation (2.3),

$$\widetilde{r}\cos\widetilde{\theta} = ar\cos\theta + br\sin\theta \quad \widetilde{r}\sin\widetilde{\theta} = cr\cos\theta + dr\sin\theta, \tag{2.5}$$

which yields

$$\widetilde{r} = r\sqrt{(a\cos\theta + b\sin\theta)^2 + (c\cos\theta + d\sin\theta)}, \quad \tan\widetilde{\theta} = \frac{c\cos\theta + d\sin\theta}{a\cos\theta + b\sin\theta}.$$

Let $\alpha(\theta) = \sqrt{(a\cos\theta + b\sin\theta)^2 + (c\cos\theta + d\sin\theta)}$. Consequently, $\widetilde{r} = \alpha(\theta)r$. Using equations (2.4)–(2.5),

$$\cos\widetilde{\theta} = \frac{a\cos\theta + b\sin\theta}{\alpha(\theta)}, \quad \sin\widetilde{\theta} = \frac{c\cos\theta + d\sin\theta}{\alpha(\theta)},$$

and, since $\widetilde{r} = \alpha(\theta)r$,

$$\begin{aligned}\widetilde{Mg_f^s(\widetilde{\theta})}\cos\widetilde{\theta} &= \alpha(\theta)Mg_f^s(\theta)\frac{a\cos\theta + b\sin\theta}{\alpha(\theta)} \\ &= aMg_f^s(\theta)\cos\theta + bMg_f^s(\theta)\sin\theta.\end{aligned}$$

Similarly, we deduce that

$$\widetilde{Mg_f^s(\widetilde{\theta})}\sin\widetilde{\theta} = cMg_f^s(\theta)\cos\theta + dMg_f^s(\theta)\sin\theta.$$

This completes the proof. □

We note that $(Mg_f^s(\theta)\cos\theta, Mg_f^s(\theta)\sin\theta)$ and $(\widetilde{Mg_f^s(\widetilde{\theta})}\cos\widetilde{\theta}, \widetilde{Mg_f^s(\widetilde{\theta})}\sin\widetilde{\theta})$ are the horizontal and vertical coordinates of the MCPT before and after the affine transform, respectively. So the above theorem shows that the MCPT can keep the affine transform relationship. For instance, Figures 2(a) and 2(b) illustrate the images of the Chinese character "Mu" and its affine transform. Figures 2(c) and 2(d) show the closed curves obtained by the MCPT of Figures 2(a), and 2(b), respectively, with different s. We observe that the closed curves extracted from the original image and the affine transformed image also satisfy the same affine transform relationship.

Lan and Yang [8] extracted affine invariant features by the CPT, the whitening transform and the Fourier transform. Affine invariants can be constructed using similar methods, but we propose a new method in this paper. The areas of closed curves derived by the MCPT are employed to construct affine invariants.

2.3. The construction of affine invariants by the MCPT By the MCPT, $Mg_f^s(\theta)$ is a closed curve in a polar coordinate system. For a complex number s, we denote

$$d^{(s)} = \frac{1}{2}\int_0^{2\pi}[Mg_f^s(\theta)]^2\,d\theta,$$

which is the area of the closed curve $Mg_f^s(\theta)$. Let $s = 2$. Then

$$d^{(2)} = \frac{1}{2}\int_0^{2\pi}[Mg_f^s(\theta)]^2\,d\theta = \frac{1}{2}\int_0^{2\pi}\int_0^{\infty} rf(r,\theta)\,dr.$$

https://doi.org/10.1017/S1446181116000341 Published online by Cambridge University Press

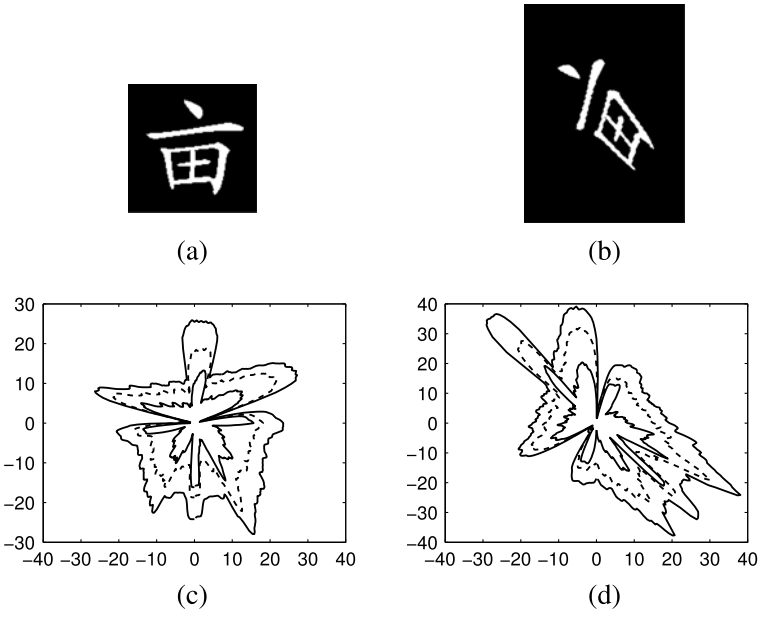

FIGURE 2. Images of a Chinese character and its affine transformation are shown in (a) and (b). The Mellin central projection transforms of the images in (a) and (b) with different values of s are shown in (c) and (d).

Note that $\int_0^{2\pi}\int_0^{\infty} rf(r,\theta)\,dr$ is the expression of the zero-order moment in the polar coordinate system.

Suppose that $f(r,\theta)$ and $\tilde{f}(\tilde{r},\tilde{\theta})$ are the original image and its affine transform, respectively. Let $Mg_f^s(\theta)$ and $\widetilde{Mg_{\tilde{f}}^s}(\tilde{\theta})$ be the MCPTs of $f(r,\theta)$ and $\tilde{f}(\tilde{r},\tilde{\theta})$, respectively. Then

$$\int_0^{2\pi}[\widetilde{Mg_f^s}(\theta)]^2 d\widetilde{\theta} = \det(A)\int_0^{2\pi}[Mg_f^s(\theta)]^2\,d\theta,$$

where $\det(A)$ is the determinant of the matrix A. Note that $d^{(s)}/d^{(2)}$ is the ratio of the area of two closed curves obtained by MCPT with different parameters. Consequently, it is affine invariant.

Let $s_1, s_2, s_3, \ldots, s_n$ be different numbers other than two. We define the vector

$$\mathbf{F} = \left[\frac{d^{(s_1)}}{d^{(2)}}, \frac{d^{(s_2)}}{d^{(2)}}, \ldots, \frac{d^{(s_n)}}{d^{(2)}}\right]^{\mathrm{T}}, \tag{2.6}$$

where T denotes the transpose of a matrix. It is also affine invariant. In the experiments, we use the vector $\mathbf{F}$ to extract invariant features of an object.

3. Experiments

In this section, we illustrate the performance of the proposed method. The first experiment is devoted to studying the invariance of the constructed affine invariants. In the second experiment, the robustness of the proposed method is tested.

https://doi.org/10.1017/S1446181116000341 Published online by Cambridge University Press

FIGURE 3. The test Chinese characters.

TABLE 1. Invariant vectors of the original images and their transformed images.

	0.8921	0.8918	0.8771	0.8778	0.9223	0.9214	0.8919	0.8921
${}^{(2+3i)}MCPT^{(2+2i)}_{(2+i)}$	0.7371	0.7372	0.7306	0.7324	0.7541	0.7514	0.7675	0.7698
	0.6646	0.6657	0.6750	0.6769	0.6558	0.6526	0.7427	0.7451
	0.3096	0.3154	0.3419	0.3464	0.2728	0.2687	0.3846	0.3930
${}^{(1.1+3i)}MCPT^{(2.5+i)}_{(2+2i)}$	0.7371	0.7372	0.7306	0.7324	0.7541	0.7514	0.7675	0.7698
	0.9763	0.9753	0.9568	0.9578	1.0241	1.0227	1.0250	1.0252
	1.0182	1.0150	0.9840	0.9853	1.1131	1.1057	1.1465	1.1444
${}^{(3.6+5i)}MCPT^{(2.8+2i)}_{(1.2+4i)}$	0.3384	0.3429	0.3482	0.3499	0.3974	0.3917	0.3949	0.3951
	0.9541	0.9529	0.9365	0.9381	1.0035	1.0011	1.0384	1.0387
	0.7393	0.7391	0.7320	0.7335	0.7854	0.7802	0.8265	0.8271
${}^{(2.3+4i)}MCPT^{(3.7+3i)}_{(1.5+i)}$	0.8124	0.8130	0.8002	0.8000	0.8243	0.8244	0.7408	0.7380
	1.0873	1.0846	1.0554	1.0570	1.1675	1.1638	1.2156	1.2138

In the following experiments, we set $n = 3$ in equation (2.6). The feature that is obtained by taking the different values s_1, s_2, s_3 is denoted by ${}^{s_3}MCPT^{s_2}_{s_1}$.

In this paper, binary images of the ten Chinese characters shown in Figure 3 are used as the test set. These images have a size of 128×128 pixels. Some of these Chinese characters have the same structure, but the shape of specific strokes of these characters may be a little different.

3.1. Affine invariance To test the affine invariance of the proposed method, vectors ${}^{(2+3i)}MCPT^{(2+2i)}_{(2+i)}$, ${}^{(1.1+3i)}MCPT^{(2.5+i)}_{(2+2i)}$, ${}^{(3.6+5i)}MCPT^{(2.8+2i)}_{(1.2+4i)}$ and ${}^{(2.3+4i)}MCPT^{(3.7+3i)}_{(1.5+i)}$ are calculated by equation (2.6) for the first four Chinese characters in Figure 3 and their affine transform images. Results are listed in Table 1. The difference of two vectors associated with two different Chinese characters is obvious, even though the characters are very similar. On the contrary, vectors associated with the original image and its affine transform image are very similar. Therefore, the vector defined in equation (2.6) is affine invariant.

https://doi.org/10.1017/S1446181116000341 Published online by Cambridge University Press

TABLE 2. The recognition accuracy for Chinese characters under different intensities of salt-and-pepper noise.

	0	0.001	0.002	0.003	0.004	0.005
${}^{(2+3i)}MCPT^{(2+2i)}_{(2+i)}$	0.9595	0.9208	0.8583	0.7976	0.7262	0.6625
${}^{(1.1+3i)}MCPT^{(2.5+i)}_{(2+2i)}$	0.9238	0.8970	0.8637	0.8405	0.8113	0.7679
${}^{(3.6+5i)}MCPT^{(2.8+2i)}_{(1.2+4i)}$	0.9690	0.9530	0.9226	0.8958	0.8518	0.8143
${}^{(2.3+4i)}MCPT^{(3.7+3i)}_{(1.5+i)}$	0.9881	0.9679	0.9399	0.8976	0.8530	0.8161
$AMIs$	0.9101	0.7161	0.6357	0.5673	0.5536	0.5232

3.2. Comparison with AMIs In this experiment, affine transformations are generated [7] by the matrix

$$A = k\begin{pmatrix}\cos\theta & -\sin\theta\\ \sin\theta & \cos\theta\end{pmatrix}\begin{pmatrix}a & b\\ 0 & \frac{1}{a}\end{pmatrix},$$

where $k \in \{0.8, 1.2\}$, $\theta \in \{30°, 90°, \ldots, 330°\}$, $b \in \{-3/2, -1, -1/2, 0, 1/2, 1, 3/2\}$ and $a \in \{1, 2\}$. As a result, every image is transformed into 168 testing images. Let η denote the classification accuracy and let $\eta = (\gamma/\tau) \times 100\%$, where γ is the number of correctly classified images and τ is the total number of images used in the test.

To reveal the robustness of affine invariants constructed by the MCPT, we compare the experimental results with the AMIs used by Flusser et al. [3]. The following three AMIs are used as affine invariant features. We denote the experiment using these quantities as AMIs.

$$AMI1 = (\mu_{20}\mu_{02} - \mu_{11}^2)/\mu_{00}^4,$$
$$AMI2 = \left\{\mu_{20}(\mu_{21}\mu_{03} - \mu_{12}^2) - \mu_{11}(\mu_{30}\mu_{03} - \mu_{21}\mu_{12}) + \mu_{02}(\mu_{30}\mu_{12} - \mu_{21}^2)\right\}/\mu_{00}^7,$$
$$AMI3 = (\mu_{30}^2\mu_{03}^2 - 6\mu_{30}\mu_{12}\mu_{21}\mu_{03} + 4\mu_{30}\mu_{12}^3 + 4\mu_{21}^3\mu_{03} - 3\mu_{21}^2\mu_{12}^2)/\mu_{00}^{10},$$

where $\mu_{i,j}$ is the central geometric moment.

Every test image had salt-and-pepper noise added with different intensities: 0, 0.001, 0.002, 0.003, 0.004, 0.005. The noise was added to the affine transformed images before recognition. The recognition accuracy for the affine invariants constructed by the proposed method and that for the AMIs are shown in Table 2. We observe that the affine invariants constructed by the proposed method have stronger robustness than the AMIs to salt-and-pepper noise.

4. Conclusion

We generalize the CPT to the MCPT in this paper. The CPT is only the accumulation of pixels along a radial direction and, inevitably, there is a loss of information. In the MCPT, a radial factor is introduced to reduce the loss of this information. Next, the Mellin transform is successfully applied to the extraction of

https://doi.org/10.1017/S1446181116000341 Published online by Cambridge University Press

affine invariant features. So far, the Mellin transform has been used only for the extraction of similar invariant features. In addition, a method is provided for the extraction of affine invariants by employing the area of the closed curves obtained by the MCPT. Experimental results demonstrate the performance of the proposed method. The MCPT can also be extended so that it can be applied to colour images [9, 10].

Acknowledgement

This work was supported in part by the National Science Foundation of China under grants 61572015, 41375115 and 11301276.

References

[1] K. Arbter, W. E. Snyder, H. Burkhardt and G. Hirzinger, "Application of affine-invariant fourier descriptors to recognition of 3-d objects", *IEEE Trans. Pattern Anal. Mach. Intell.* **12** (1990) 640–647; doi:10.1109/34.56206.

[2] F. Bouyachchera, B. Boualia and M. Nasri, "Clifford Fourier–Mellin moments and their invariants for color image recognition", *Math. Comput. Simulation* **40** (2014) 27–35; doi:10.1016/j.matcom.2014.11.005.

[3] J. Flusser, T. Suk and B. Zitov¢, *Moments and moment invariants in pattern recognition* (John Wiley and Sons, Chichester, UK, 2009); https://www.amazon.com/Moments-Moment-Invariants-Pattern-Recognition/dp/0470699876.

[4] L. Guo and M. Zhu, "Quaternion Fourier–Mellin moments for color images", *Pattern Recognit.* **44** (2011) 187–195; doi:10.1016/j.patcog.2010.08.017.

[5] M. Hazewinkel (ed.), "Mellin transform" in: *Encyclopedia of mathematics,* Volume 6 (Kluwer Academic Publishers, Dordrecht, The Netherlands, 1990); http://www.encyclopediaofmath.org/index.php?title=Mellin_transform&oldid=36080.

[6] T. V. Hoang and S. Tabbone, "Invariant pattern recognition using the rfm descriptor", *Pattern Recognit.* **45** (2012) 271–284; doi:10.1016/j.patcog.2011.06.020.

[7] M. I. Khalil and M. M. Bayoumi, "A dyadic wavelet affine invariant function for 2d shape recognition", *IEEE Trans. Pattern Anal. Mach. Intell.* **23** (2001) 1152–1163; doi:10.1109/34.954605.

[8] R. S. Lan and J. W. Yang, "Whitening central projection descriptor for affine-invariant shape description", *IET Image Process.* **7** (2013) 81–91; doi:10.1049/iet-ipr.2012.0094.

[9] R. S. Lan and Y. Ch. Zhou, "Quaternion-Michelson descriptor for color image classification", *IEEE Trans. Image Process.* **25** (2016) 5281–5292; doi:10.1109/TIP.2016.2605922.

[10] R. S. Lan, Y. Ch. Zhou and Y. Y. Tang, "Quaternionic local ranking binary pattern: a local descriptor of color images", *IEEE Trans. Image Process.* **25** (2016) 566–579; doi:10.1109/TIP.2015.2507404.

[11] J. Mennesson, C. Saint-Jean and L. Mascarilla, "Color fouriercmellin descriptors for image recognition", *Pattern Recognit. Lett.* **40** (2014) 27–35; doi:10.1016/j.patrec.2013.12.014.

[12] Y. Y. Tang, Y. Tao and E. C. M. Lam, "New method for extraction based on fractal behavior", *Pattern Recognit.* **35** (2002) 1071–1081; doi:10.1016/S0031-3203(01)00095-4.

[13] C. Teh and R. Chin, "On image analysis by methods of moments", *IEEE Trans. Pattern Anal. Mach. Intell.* **10** (1988) 496–513; doi:10.1109/34.3913.